Short distance constraints from HLbL contribution to the muon anomalous magnetic moment

Daniel Gerardo Melo Porras[a]

In collaboration with:

Angelo Raffaele Fazio[a], Edilson Alfonso Reyes Rojas[b]

[a]Universidad Nacional de Colombia, [b]Universidad de Pamplona

Conference in High Energy Physics,
A.I. Alikhanyan National Science Laboratory

Yerevan, Armenia
September 14, 2023

Outline

1. Status of the $(g-2)_\mu$
2. HLbL scattering: The basics
3. OPE for $\Pi^{\mu_1\mu_2\mu_3\mu_4}$
4. Quark loop computation
5. Conclusions

Outline for section 1

What is a_μ?

Magnetic moment: $\boldsymbol{\mu} = g\frac{q}{2m}\boldsymbol{S}$

From Dirac's equation:

$g = 2$

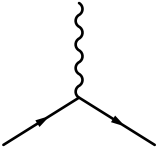

But quantum particles introduce an anomaly:

$$a = \frac{g-2}{2}$$

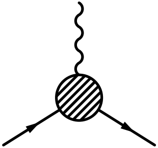

Why is a_μ relevant today?

D. P. Aguillard et al. arXiv:2308.06230

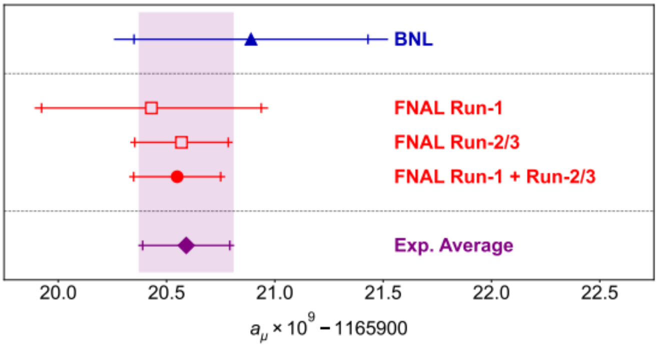

Why is a_μ relevant today?

Difference between Standard Model (SM) prediction and measurement:

$$\Delta a_\mu = a_\mu^{\text{exp}} - a_\mu^{\text{WP}} = \boxed{249\,(48) \times 10^{-11}} \text{ or } 5.2\,\sigma(?)$$

Experimental values $[10^{-11}]$		
a_μ^{BNL}	=	116 592 089 (63)
a_μ^{FNAL}	=	116 592 055 (24)
a_μ^{exp}	=	116 592 059 (22)
Future:	=	... (16)

SM consensus $[10^{-11}]$		
a_μ^{WP}	=	116 591 810 (43)

T. Aoyama et al. (2020)

Where does a_μ^{WP} come from?

Theoretical prediction must keep up with Fermilab and J-PARC's projected uncertainty reductions.

Where can this reduction come from?

- QED gives the largest contribution, but its uncertainty is under control for the forseeable future.
- EW contributions small and uncertainty also under control.

Where does a_μ^{WP} come from?

Hadronic vacuum polarization (HVP) up to NNLO.

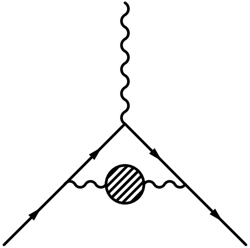

Hadronic Light–by–Light scattering (HLbL) up to NLO.

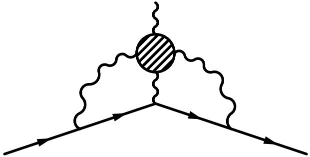

Where does a_μ^{WP} come from?

- The hadronic part has the largest uncertainty:

$$a_\mu^{\text{HVP}} = 6\,845\,(40) \times 10^{-11} \qquad \text{(data–driven)}$$
$$a_\mu^{\text{HLbL}} = 92\,(18) \times 10^{-11}$$

- HVP is the biggest uncertainty (and trouble!) source.
- HLbL has the largest relative uncertainty of any of the main contributions!

HVP: lattice, dispersive and experiments

S. Kuberksi, talk at the Sixth Plenary Workshop of the Muon $g-2$ Theory Initiative, Bern University, September 4th – 8th, 2023

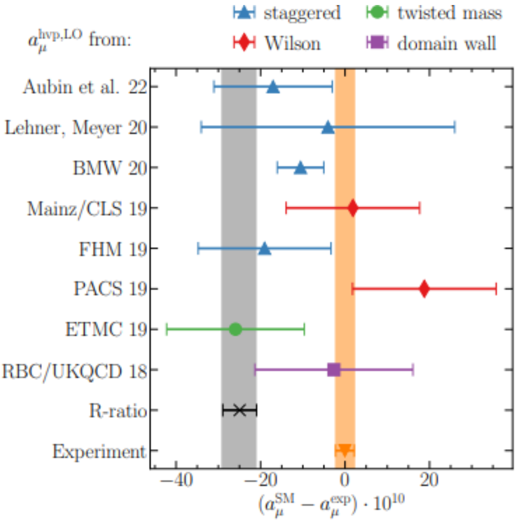

$a_\mu^{\pi\pi}$ HVP: lattice, dispersive and experiments

M. Davier, talk at the Sixth Plenary Workshop of the Muon $g-2$ Theory Initiative, Bern University, September 4th – 8th, 2023

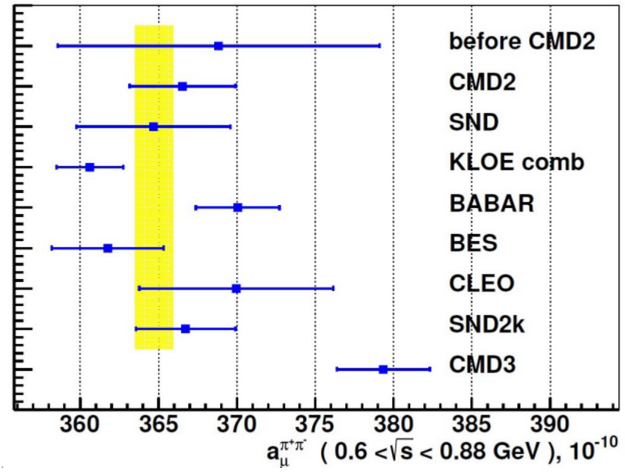

Outline for section 2

Basics of $\Pi^{\mu_1\mu_2\mu_3\mu_4}$

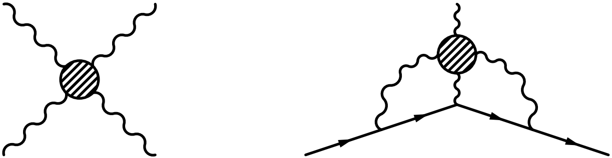

$$\Pi^{\mu_1\mu_2\mu_3\mu_4} = -i\int d^4x\int d^4y\int d^4z\, e^{-i(q_1x+q_2y+q_3z)}$$
$$\times\langle\Omega|J^{\mu_1}(x)J^{\mu_2}(y)J^{\mu_3}(z)J^{\mu_4}(0)|\Omega\rangle$$

➥ Loops on q_1 and q_2 sweep very different kinematic regions. Alternate tools required near Λ_{QCD} and below it.

Dispersive computation of $\Pi^{\mu_1\mu_2\mu_3\mu_4}$

Analyticity: (Sugawara–Kanazawa + Mandelstam hypothesis)

$$g(z) = \sum_i \frac{R_i}{z-x_i} + \frac{1}{\pi}\left(\int_{c_1}^{\infty} + \int_{-\infty}^{-c_2}\right)\frac{\Delta_x g(x)}{x-z}\,dx + \lim_{x\to\infty}\overline{g}(x)$$

$$\Delta_x g(x) = \frac{1}{2i}\{g(x+i\epsilon) - g(x-i\epsilon)\}$$

$$\overline{g}(x) = \frac{1}{2}\{g(x+i\epsilon) + g(x-i\epsilon)\}$$

Unitarity:

Schwarz: $\mathrm{Im}\, g \to \Delta_x g$

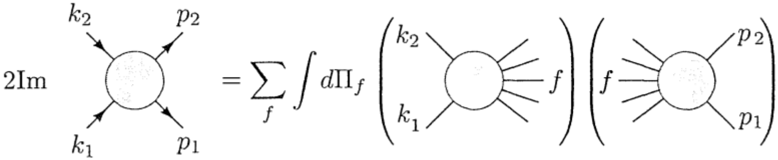

Dispersive computation of $\Pi^{\mu_1\mu_2\mu_3\mu_4}$

The "basis" of $\Pi^{\mu_1\mu_2\mu_3\mu_4}$ free of kinematic singularities and zeroes:

$$\Pi^{\mu_1\mu_2\mu_3\mu_4} = \sum_i^{54} \Pi_i T_i^{\mu_1\mu_2\mu_3\mu_4}$$

Colangelo et al. (2017)

- From 138 to 43 independent tensors vs. 1 in HVP.
- To avoid kinematic zeroes/singularities it is necessary to expand to 54 redundant Π_i. (Tarrach)
- Richer tensor structure made BTT basis much harder to find.

Low energy, data–driven a_μ^{HLbL}

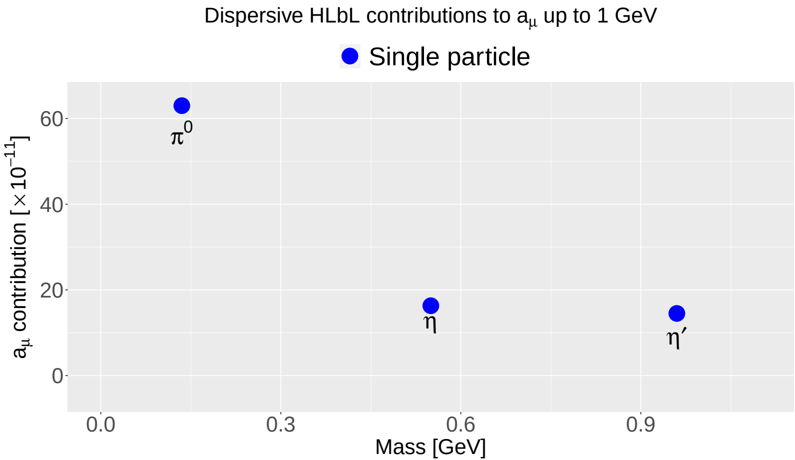

Low energy, data–driven a_μ^{HLbL}

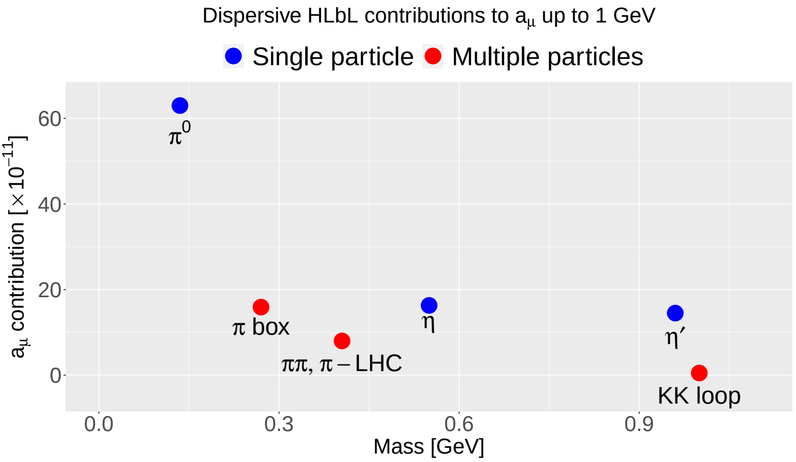

Estimation of a_μ^{HLbL} in 1 GeV − 2 GeV

Hurdles for dispersive computation in the medium–energy region:

- Lack of data for: known form factors at high energy. and new unknown form factors.
- Increasing complexity of unitarity diagrams.
- Double counting issues.

The expected small size of contributions motivates narrow width approximation, which results in:

$$a_\mu^{\text{scalars+tensor}} = -1(3)\times 10^{-11}$$
$$a_\mu^{\text{axial vectors}} = 6(6)\times 10^{-11}$$

a_μ^{HLbL} at high energy and SDC

SDC = asymptotic behaviour of amplitudes.

Useful for:

- High energy contributions from light intermediate states. (Form factors)
- Full contributions from heavy intermediate states. (HLbL amplitude)

We focus in the latter case!

Two high virtualities regimes:

$$|q_1^2| \sim |q_2^2| \sim |q_3^2| \gg \Lambda_{\text{QCD}}^2 \qquad |q_1^2| \sim |q_2^2| \gg |q_3^2|, \Lambda_{\text{QCD}}^2$$

Outline for section 3

Symmetric asymptotic limit for $\Pi^{\mu_1\mu_2\mu_3\mu_4}$

- The OPE is an useful tool, meant for high energies, so one must be careful.
- Four–current OPE not suitable due to soft external photon:
- Mix of different scales is very problematic in QCD.

Bijnens et al.(2019, 2020, 2021) solved this with an OPE with a background soft photon for:

$$\Pi^{\mu_1\mu_2\mu_3} = \frac{1}{e}\langle\Omega|J^{\mu_1}(q_1)J^{\mu_2}(q_2)J^{\mu_3}(0)|\gamma(q_4)\rangle$$
$$= -\epsilon_{\mu_4}(q_4)\Pi^{\mu_1\mu_2\mu_3\mu_4}(q_1,q_2,q_3)\ ,$$

OPE elements for $\Pi^{\mu_1\mu_2\mu_3}$

List of OPE elements:

$$S_{1,\mu\nu} \equiv ee_f F_{\mu\nu} \,,$$
$$S_{2,\mu\nu} \equiv \overline{\Psi}\sigma_{\mu\nu}\Psi \,,$$
$$S_{3,\mu\nu} \equiv ig_S\overline{\Psi}G_{\mu\nu}\Psi \,,$$
$$S_{4,\mu\nu} \equiv ig_S\overline{\Psi}\,\overline{G}_{\mu\nu}\gamma_5\Psi \,,$$
$$S_{5,\mu\nu} \equiv \overline{\Psi}\Psi\; ee_f F_{\mu\nu} \,,$$

$$S_{6,\mu\nu} \equiv \frac{\alpha_s}{\pi} G_a^{\alpha\beta} G^a_{\alpha\beta}\; ee_f F_{\mu\nu} \,,$$
$$S_{7,\mu\nu} \equiv g_S\overline{\Psi}(G_{\mu\lambda}D_\nu + D_\nu G_{\mu\lambda})\gamma^\lambda\Psi + g_S\overline{\Psi}(G_{\nu\lambda}D_\mu + D_\mu G_{\nu\lambda})\gamma^\lambda\Psi \,,$$
$$S_{\{8\},\mu\nu} \equiv \alpha_s(\overline{\Psi}\Gamma\Psi\overline{\Psi}\Gamma\Psi)_{\mu\nu} \,,$$

Same quantum numbers as $F_{\mu\nu}$:

- ➥ Second rank
- ➥ Antisymmetric
- ➥ Odd C–parity

Outline for section 4

The quark loop

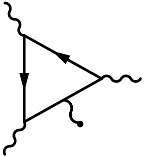

$$S_{1,\mu\nu} \to \Delta a_\mu^{HLbL} = 1.7 \times 10^{-10}$$
$$S_{2,\mu\nu} \to \Delta a_\mu^{HLbL} = -1.2 \times 10^{-12}$$
$$\ldots$$

Wilson coefficient of $\langle F_{\mu\nu} \rangle$, proportional to:

$$i\frac{N_c}{2}\int \frac{d^4p}{(2\pi)^4}\frac{\partial}{\partial q_{4\nu_4}}\sum_{\sigma(1,2,4)}\left\{\gamma^{\mu_3}S^0(p+q_1+q_2+q_4)\gamma^{\mu_4}\right.$$
$$\left.\times S^0(p+q_1+q_2)\gamma^{\mu_1}S^0(p+q_2)\gamma^{\mu_2}S^0(p)\right\}\Big|_{q_4=0}$$

S^0 is the free fermion propagator. Due to mixing, its massless part is the real LO of the OPE.

Quark loop computation

Bijnens (2020) uses the standard approach:

- Project $\overline{\Pi}_i$ out of the quark loop and compute the rest.
- Taylor expand massive propagators.
- Use Integration By Parts (IBP) to arrive at a small number of master integrals.

Quark loop computation

We tensor decompose the quark loop amplitude following Davydychev (1991), for instance

$$
\begin{aligned}
I^{(2)}_{\mu_1\mu_2}(d;\nu_1,\nu_2) = &-\frac{1}{2\pi} g_{\mu_1\mu_2} I^{(2)}(d+2;\{\nu_i\}) \\
&+ \frac{1}{\pi^2} q_{1\mu_1} q_{1\mu_2} \nu_1(\nu_1+1) I^{(2)}(d+4;\nu_1+2,\nu_2) \\
&+ \frac{1}{\pi^2} q_{2\mu_1} q_{2\mu_2} \nu_2(\nu_2+1) I^{(2)}(d+4;\nu_1,\nu_2+2) \\
&+ \frac{1}{\pi^2} (q_{1\mu_1} q_{2\mu_2} + q_{1\mu_2} q_{2\mu_1}) \nu_1\nu_2 I^{(2)}(d+4;\nu_1+2,\nu_2+1)
\end{aligned}
$$

It does not introduce kinematic singularities, but at the cost of shifting dimensions.

Superficial degree of divergence conserved!

Scalar integrals in shifted dimensions

We find 133 different scalar triangle and self–energy integrals in shifted dimensions.

Davydychev (1991) gives Mellin–Barnes (MB) representation for arbitrary scalar integrals:

$$I^{(2)}(d;\nu_1,\nu_2) = \int_{s_1}\left(-\frac{q_1^2}{m^2}\right)^{s_1}\Gamma(-s_1)\frac{\Gamma(s_1+\nu_1)\Gamma(s_1+\nu_2)}{\Gamma(2s_1+\nu_1+\nu_2)} \times\Gamma\left(s_1+\nu_1+\nu_2-\frac{d}{2}\right)$$

Scalar integrals in shifted dimensions

Usual Taylor expansion of massive propagators:

$$\frac{1}{(p^2-m^2)^\nu} = \frac{1}{p^{2\nu}}\frac{1}{\Gamma(\nu)}\sum_{n=0}\frac{1}{n!}\left(\frac{m^2}{p^2}\right)^n\Gamma(\nu+n) \qquad \text{for} \qquad \left|\frac{m^2}{p^2}\right|<1\,,$$

$$= \frac{1}{(-m^2)^\nu}\frac{1}{\Gamma(\nu)}\sum_{n=0}\frac{1}{n!}\left(\frac{p^2}{m^2}\right)^n\Gamma(\nu+n) \qquad \text{for} \qquad \left|\frac{p^2}{m^2}\right|<1\,.$$

MB representation is valid for any kinematic regime:

$$\frac{1}{(p^2-m^2)^\nu} = \frac{1}{m^{2\nu}}\frac{1}{\Gamma(\nu)}\int_{-i\infty}^{i\infty} ds\left(-\frac{p^2}{m^2}\right)^s\Gamma(\nu+s)\Gamma(-s)\,.$$

Full mass dependence conserved.

Scalar integrals in shifted dimensions

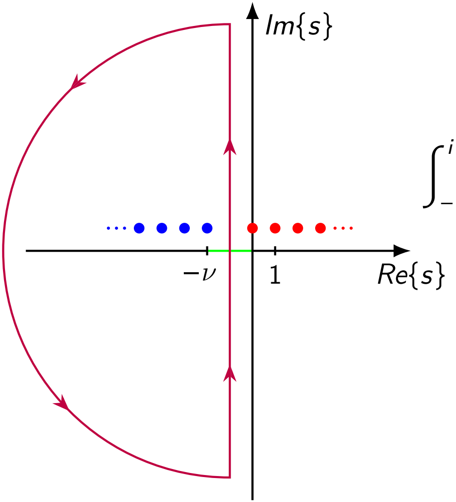

$$\int_{-i\infty}^{i\infty} ds \left(-\frac{p^2}{m^2}\right)^s \Gamma(\nu+s)\Gamma(-s)$$

$$\left|\frac{m^2}{p^2}\right| < 1 \qquad \left|\frac{p^2}{m^2}\right| < 1$$

Scalar integrals in shifted dimensions

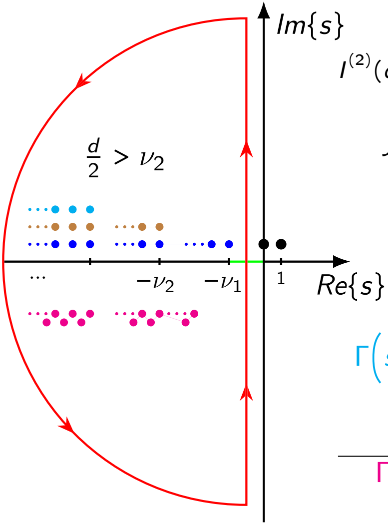

$$I^{(2)}(d;\nu_1,\nu_2) = \int_{s_1}\left(-\frac{q_1^2}{m^2}\right)^{s_1}\Gamma(-s_1)\frac{\Gamma(s_1+\nu_1)\Gamma(s_1+\nu_2)}{\Gamma(2s_1+\nu_1+\nu_2)} \times\Gamma\left(s_1+\nu_1+\nu_2-\frac{d}{2}\right)$$

$$\frac{\Gamma\left(s+\nu_1+\nu_2-\frac{d}{2}\right)\;\Gamma(s+\nu_2)\;\Gamma(s+\nu_1)}{\Gamma(2s+\nu_1+\nu_2)} \quad \Big| \quad \Gamma(-s)$$

Scalar integrals in shifted dimensions

Nested MB integrals require multivariate residues (*MBConicHulls (B. Ananthanarayan et al, 2021)*, *Multivariate residues (Larsen, 2017)*)

- ➥ There are several different triple (almost) hypergeometric series representation for one integral.
- ➥ Convergence of hypergeometric series studied with Horn's theorem.
- ➥ Too many integrals with too many representations: We wrote a script to check the convergence region of series representations.

Scalar integrals in shifted dimensions

Two–point example for $|q^2| > 4m^2$:

$$
\begin{aligned}
I^{(2)}(6;\nu,\nu+1) &= \frac{-i}{(4\pi)^{5/2}}\frac{(m^4)^{1-\nu}}{\Gamma(\nu)\Gamma(\nu+1)} \\
&\times\Bigg\{\Big(-\frac{4m^2}{q^2}\Big)^{\nu}\sum_{k=0}^{\nu-3}\Big(\frac{4m^2}{q^2}\Big)^{k}\frac{\Gamma(\nu+k)}{\Gamma(-k+\frac{1}{2})}\frac{\Gamma(-k+\nu-2)}{\Gamma(k+1)} \\
&-\Big(-\frac{16m^4}{q^4}\Big)^{\nu-1}\sum_{l=0}^{\infty}\Big(-\frac{4m^2}{q^2}\Big)^{l}\frac{\Gamma(-2+2\nu+l)}{\Gamma(-\nu-l+\frac{5}{2})}\frac{1}{\Gamma(l+1)\Gamma(l+\nu-1)} \\
&\times\Bigg(\ln\Big\{-\frac{q^2}{4m^2}\Big\}-\psi^{(0)}(-2+2\nu+l)-\psi^{(0)}(-\nu-l+\frac{5}{2})-3\psi^{(0)}(l+1) \\
&\qquad+\psi^{(0)}(l+\nu-1)\Bigg)\Bigg\}
\end{aligned}
$$

Check of BTT tensor decomposition of $\Pi^{\mu_1\mu_2\mu_3\mu_4}$

$$\left.\frac{\partial \Pi^{\mu_1\mu_2\mu_3\mu_4}}{\partial q_{4\mu_5}}\right|_{q_4\to 0} = \sum_i^{19} \Pi_i \, \partial^{\mu_5} T_i^{\mu_1\mu_2\mu_3\mu_4}\Big|_{q_4\to 0}$$

- All form factors receive contributions from the quark loop? (Weak)

$$\Pi_i \neq 0$$

- Are there contributions to tensor structures not considered in BTT? (Strong)

$$\left.\frac{\partial \Pi^{\mu_1\mu_2\mu_3\mu_4}}{\partial q_{4\mu_5}}\right|_{q_4\to 0} - \sum_i^{19} \Pi_i \, \partial^{\mu_5} T_i^{\mu_1\mu_2\mu_3\mu_4}\Big|_{q_4\to 0} = 0$$

Outline for section 5

Conclusions

Main contributions:

- Independent check for the quark loop computation.
- Check of the complete span of the dispersive tensor basis for the quark loop amplitude.
- Complement for the *MBConicHulls* Mathematica package to automatize the study of convergence regions of multiple variables (almost) hypergeometric series.

Perspectives

Perspectives:

- Further perturbative corrections to $O(\alpha_S^2)$. Already done at $O(\alpha_S)$ by Bijnens et al. (2021)
- OPE for the HLbL tensor in the mixed–virtualities asymptotic regime. Axial anomaly gives lowest dimensional operator. Work in progress by Bijnens et al. (2023)

Thanks!